BT8009; A Nectin-4 Targeting Bicycle Toxin Conjugate for Treatment of Solid Tumors

Michael Rigby[1], Gavin Bennett[1], Liuhong Chen[1], Gemma E. Mudd[1], Helen Harrison[2], Paul J. Beswick[1], Katerine Van Rietschoten[1], Sophie M. Watcham[3], Heather S. Scott[1], Amy N. Brown[1], Peter U. Park[4], Carly Campbell[5], Eric Haines[6], Johanna Lahdenranta[5], Michael J. Skynner[1], Phil Jeffrey[1], Nicholas Keen[5], and Kevin Lee[1]

ABSTRACT

Multiple tumor types overexpress Nectin-4 and the antibody–drug conjugate (ADC), enfortumab vedotin (EV) shows striking efficacy in clinical trials for metastatic urothelial cancer, which expresses high levels of Nectin-4, validating Nectin-4 as a clinical target for toxin delivery in this indication. Despite excellent data in urothelial cancer, little efficacy data are reported for EV in other Nectin-4 expressing tumors and EV therapy can produce significant toxicities in many patients, frequently leading to discontinuation of treatment. Thus, additional approaches to this target with the potential to extend utility and reduce toxicity are warranted. We describe the preclinical development of BT8009, a "*Bicycle* Toxin Conjugate" (BTC) consisting of a Nectin-4–binding bicyclic peptide, a cleavable linker system and the cell penetrant toxin monomethylauristatin E (MMAE). BT8009 shows significant antitumor activity in preclinical tumor models, across a variety of cancer indications and is well tolerated in preclinical safety studies. In several models, it shows superior or equivalent antitumor activity to an EV analog. As a small hydrophilic peptide-based drug BT8009 rapidly diffuses from the systemic circulation, through tissues to penetrate the tumor and target tumor cells. It is renally eliminated from the circulation, with a half-life of 1–2 hours in rat and non-human primate. These physical and PK characteristics differentiate BT8009 from ADCs and may provide benefit in terms of tumor penetration and reduced systemic exposure. BT8009 is currently in a Phase 1/2 multicenter clinical trial across the US, Canada, and Europe, enrolling patients with advanced solid tumors associated with Nectin-4 expression.

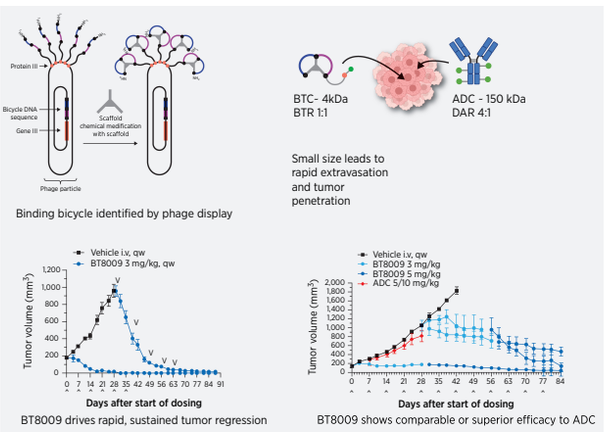

Introduction

The principle of tumor-targeted delivery of cytotoxic agents is now well established through antibody–drug conjugates (ADC). Despite encouraging preclinical data, in many cases ADCs have failed to fulfill their promise in clinical trials. In the 20 years since the accelerated approval of gentuzumab ozogamicin, there have only been a further 11 FDA-approved ADCs, with just 5 being approved for solid tumors. It has been hypothesized that imperfect translation from preclinical species to human is in part driven by both poor tumor penetration, and the intrinsically long half-life (days to weeks) of ADCs leading to non-tumor deposition of payload. Although antibodies provide a high-affinity and high-specificity carrier for toxin delivery, their large molecular size (∼150 kDa) impedes their ability to overcome the combined obstacles of the endothelial barrier, interstitial pressure and the complex stromal structure present in tumors. This results in low extravasation rates and slow diffusion through the extracellular compartment. As little as 0.01%–0.1% of injected antibody may reach solid tumor antigens (1). High antigen expression and subsequent ADC internalization in the perivascular regions of the tumor contribute to the formation of a "binding site barrier" (2, 3) further hindering penetration to poorly perfused regions of the tumor. Counterintuitively *in vitro* and *in vivo* studies show that coadministration of trastuzumab with ado-trastuzumab emtansine improves the ADC efficacy in tumor models (4–6) presumably by reducing binding of ADC at the binding site barrier allowing enhanced ADC penetration into the tumor. This observation also supports the suggestion that tumor cells proximal to the vasculature take up more toxin than is required to initiate cell death (because efficacy is not reduced by target blockade), depleting toxin availability for more distal cells.

To overcome poor tumor penetration, the ADC dose can be increased, but this carries with it increased safety liability. Alternatively, the toxin load can be increased with increased drug–antibody ratios (DAR) of >3 being common, but this risks increased toxin exposure to normal tissue with associated safety liabilities, while

[1]Bicycle TX Ltd., Cambridge, United Kingdom. [2]Amphista Therapeutics, The Cori Building, Cambridge, United Kingdom. [3]Kymab Ltd., The Bennet Building, Babraham Research Campus, Cambridge, United Kingdom. [4]Orum Therapeutics, Cambridge, Massachusetts. [5]Bicycle Therapeutics, Inc., Lexington, Massachusetts. [6]Ikena Oncology, Boston, Massachusetts.

Corresponding Author: Michael Rigby, Bicycle TX Ltd., Blocks A & B, Portway Building, Granta Park, Cambridge, CB21 6GP, UK. Phone: 44-012-2326-1512; E-mail: mike.rigby@BicycleTX.Com

Mol Cancer Ther 2022;21:1747–56

doi: 10.1158/1535-7163.MCT-21-0875

This open access article is distributed under the Creative Commons Attribution-NonCommercial-NoDerivatives 4.0 International (CC BY-NC-ND 4.0) license.

©2022 The Authors; Published by the American Association for Cancer Research

further overdosing tumor cells proximal to the vasculature. An argument can be made for reducing DAR, while delivering more toxin carrying molecules, to maintain the same overall total toxin delivery (4).

Therapeutic index for ADCs could also be improved by reduced duration of systemic exposure to reduce adverse toxicities. ADCs show systemic half-lives typically in the range 3–6 days (7) and this longer exposure may compensate for their poor tissue penetration. However, extended exposure can subject them to circulating plasma proteases permitting gradual systemic payload release (8) and makes them more liable to non-specific internalization into off target tissues through macro/micropinocytosis or off tumor target, but antibody-specific receptor–mediated uptake (e.g., Fc receptors or C type lectin receptors; refs. 9, 10). Improving tumor penetration may allow shorter systemic exposure to reduce off target toxicities while maintaining efficacy.

The opportunity, therefore, exists to enhance the therapeutic index of targeted delivery of toxins by improving extravasation and diffusion to the tumor cell (including minimizing impact of the binding site barrier) to increase efficacy, while simultaneously shortening duration of systemic exposure to reduce systemic toxicity.

The cell adhesion molecule Nectin-4 shows elevated expression in multiple tumor types (11–13) correlated with poor prognosis (14–16). Nectin-4–directed ADCs show efficacy in multiple xenograft tumor models (13, 17). The ADC enfortumab vedotin (EV) delivers the antimitotic toxin MMAE to Nectin-4–expressing cells via internalization and cleavage of a valine–citrulline dipeptide linker component (18). Clinical validation of Nectin-4 as a target in urothelial cancer has been demonstrated with EV. In 2021, the FDA-approved EV for patients with locally advanced or metastatic urothelial cancer who had previously received a PD-1 or PD-L1 inhibitor and platinum-containing chemotherapy or were ineligible for cisplatin containing chemotherapy and had received one or more prior lines of therapy.

Bicycle toxin conjugates (BTC) are structurally constrained bicyclic peptides conjugated through cleavable linkers to a toxin. Various, well-described linker toxin combinations can be incorporated into the BTC molecule (e.g., BT1718 and BT5528; refs. 19–20). They are of low molecular weight (approximately 4–4.5 kDa) and being chemically synthesized can be optimized for appropriate affinity, stability, and solubility relatively simply. Through intravenous administration, high systemic C_{max} values can be attained, which, along with BTCs' relatively small size, helps drive rapid diffusion into extra-vascular compartment, as reflected in a volume of distribution similar to extracellular fluid. We believe that delivery of a high number of BTCs, each carrying a reduced toxin load (peptide toxin ratio of 1:1) should improve tumor penetration and reduce the impact of the "binding site barrier." BTCs show moderate clearance from the systemic vasculature, predominantly by the renal route. This overall profile marks them out from most ADCs and provides the possibility of enhanced clinical efficacy with a wider therapeutic index.

In this report, we describe the characteristics of BT8009, a Nectin-4–targeting BTC in which a Nectin-4–binding peptide with a sarcosine decamer spacer is conjugated to the cell penetrant toxin MMAE by a valine–citrulline cleavable linker; the same toxin linker combination present in EV. The sarcosine spacer is designed to reduce steric hindrance by the Bicycle of enzymatic linker cleavage. BT8009 has a molecular mass of 4171 and a peptide toxin ratio of 1:1, MMAE can be liberated by proteases (e.g., cathepsin B) elevated in the tumor microenvironment (TME), without necessarily the requirement for internalization. This capacity for TME cleavage and toxin release plays to the strengths of the cell permeant toxin MMAE, in killing tumor cells and through bystander killing of adjacent stromal cells, which may contribute to more rapid tumor regression. In addition, there is increasing evidence that ADC resistance may arise through changes in antigen internalization, changes in endocytic/lysosomal processing or liberated toxin release from the lysosome into the cytoplasm (21–23). Because BTCs do not necessarily require internalization for toxin release they may avoid these resistance mechanisms.

BT8009 evokes robust tumor regression in multiple xenograft models expressing Nectin-4 and can be administered in a range of dosing paradigms. The PK data show it has a moderate volume of distribution, moderate plasma clearance, and a short plasma terminal half-life with low plasma levels of unconjugated MMAE, Tumor penetration of MMAE is significant and is retained long after both parent and toxin are cleared from systemic circulation.

Materials and Methods

Phage optimization of nectin-4–binding peptides

Bicycles binding Nectin-4 were selected by phage display using Materials and Methods described previously by Heinis and colleagues (24) and were subsequently chemically optimized (further details are provided in the Supplementary Material).

In vitro studies

Binding affinities were determined using a fluorescence polarization assay during the early-screening phase and later by surface plasmon resonance (SPR) using conventional methods in which protein is coated on the chip and test agent passed over it. SPR was used to determine affinities against Nectin-4 from human and toxicology species, and to assess selectivity against other human Nectin and Nectin-like family members. Affinity of the Nectin-4 ADC was measured, using SPR, by coating a chip with ADC and passing protein sample over it. Functional interaction with several human cardiac ion channels was assessed in electrophysiological patch clamp studies (Metrion Biosciences Ltd.).

Selectivity of the biotinylated Bicycle binder (BCY9565) present in BT8009 was assessed in a Retrogenix assay against 5,528 human full-length human plasma membrane proteins and secreted proteins expressed in HEK293 cells (Retrogenix Ltd.). The 5,528 proteins present in this assay are listed in the Supplementary Data.

Cell binding of BT8009 to endogenous nectin-4

BT8009 binding to live cells expressing Nectin-4 was assessed by high content imaging. Cells were incubated with one of: BT8009, the Nectin-4 ADC, a non-binding BTC (BCY8781), or MMAE for 45 minutes at 4°C followed by washing. Binding of the BTC or ADC was visualized using an anti-MMAE antibody conjugated to fluorescein. A membrane marker was included to assist membrane localization and cell nuclei were stained with DAPI.

Nectin-4 expression on human cell lines

Nectin-4 expression was assessed in several cell or patient derived tumor samples by measurement of Nectin-4 antibody binding to isolated cells using flow cytometry. In some studies, absolute antibody-binding sites were quantified using Quantibrite Beads.

Plasma protein binding, stability in plasma, and hepatocytes

Plasma protein binding and plasma stability were assessed in plasma from CD1 mouse, Sprague–Dawley rat, cynomolgus monkey and human. Stability was also assessed in hepatocytes and microsomes from CD1 mouse, Sprague–Dawley rat, cynomolgus monkey and human. Studies were conducted at WuXi AppTec using conventional protocols.

Quantifying BT8009 and MMAE in plasma and tumor

BT8009 and MMAE levels were quantified in plasma and tumor samples following analyte extraction and bioanalysis using LC/MS-MS assays.

Xenograft models

Cell-derived xenograft (CDX) studies were conducted in BALB/c nude, or CB17-SCID mice inoculated with approximately 10^7 cells in the right flank. All studies included a vehicle-treated control. For patient-derived xenograft (PDX) models a tumor fragment (~30 mm^3) was implanted in the right flank. Tumor volumes were measured using calipers, and the volume calculated. These xenograft studies were conducted at WuXi AppTec (Shanghai, China).

Further PDX xenograft studies were performed at Champions Oncology, Inc. (Hackensack), in 6- to 8-week-old female athymic Nude-*Foxn1*^{nu} mice implanted with a tumor fragment in the left flank. Tumor volumes were measured using calipers and tumor volume calculated.

Dosing was by intravenous bolus in all studies, routinely at weekly intervals (qw), although in some studies regimens of twice weekly (biw) or once every two weeks (q2w) were also used.

All the procedures related to animal handling, care, and treatment in the studies were performed according to the guidelines approved by the Institutional Animal Care and Use Committee (IACUC) of WuXi AppTec (Shanghai, China) or Champions Oncology (Hackensack), following the guidance of the Association for Assessment and Accreditation of Laboratory Animal Care.

General toxicology studies

In accordance with the recommendations of ICH S9 Nonclinical Evaluation of Anticancer Pharmaceuticals, general toxicology studies were conducted at Labcorp Early Development Laboratories (formerly Envigo Ltd.), Huntingdon, UK. Studies were conducted in an AAALAC accredited facility in alignment with applicable animal welfare regulations and in accordance with Good Laboratory Practice regulations. Repeat dose studies with BT8009 were performed in rat (1, 3, and 5 mg/kg/occasion) and non-human primate (cynomolgus monkey; 0.25, 0.5, and 0.75 mg/kg/occasion). BT8009 was administered via a short (15 minutes) intravenous infusion once weekly for 5 doses on days 1, 8, 15, 22, and 29, over a 32-day period. Evaluations included clinical signs, body weight and food consumption, macroscopic and microscopic pathology, hematology, clinical chemistry, urinalysis, coagulation and toxicokinetics (conjugate and payload).

Data availability

All data relevant to the studies are included in the article or uploaded as online Supplementary Information. The datasets used and analyzed during these studies are available from the corresponding author on reasonable request.

Results

Generation of high-affinity Nectin-4 BTC and comparator molecules (Nectin-4 ADC, non-binding BTC)

Bicyclic Nectin-4 binders were identified using proprietary phage display technology (24) providing a preliminary binding sequence with low nmol/L affinity but having poor *in vitro* plasma stability and solubility. These initial phage display leads were subsequently chemically optimized as described previously in another article (25). The resultant binding peptide, BCY8126, showed good solubility and high affinity for human, NHP, rat and mouse Nectin-4. *In vitro* stability was improved in mouse, NHP and human plasma. BCY8126 was selected as the Nectin-4–binding peptide to be incorporated into the BTC. For BTC generation, the 26 amino acid linear peptide, comprising the peptide binder and the sarcosine decamer molecular spacer, was synthesized using solid phase peptide synthesis, followed by cyclization using TATA (1,3,5-Triacryloylhexahydro-1,3,5-triazine). In a separate step, the toxin and linker component were synthesized (glutaric acid-valine-citrulline-PABC-MMAE) and subsequently conjugated to the beta alanine N-terminus of the sarcosine spacer.

A Nectin-4 comparator ADC was generated on the basis of published data for EV. The antibody was generated by GenScript USA, Inc.; ADC generation was performed at WuXi Biologics providing a Nectin-4 ADC with a molecular weight of 152kDa and a DAR of 3.98, consistent with EV. In this publication "Nectin-4 ADC" refers to this EV analog. The Nectin-4 ADC–bound Nectin-4 with a K_D value from 1.2 to 4.6 nmol/L by SPR.

Substitution of two key-binding residues of the BCY8126 peptide (L-Trp replaced with D-Trp) generated the non-binding BTC, BCY8781, with comparable physicochemical properties with BT8009, but lacking affinity for Nectin-4.

Structures of BT8009, the non-binding control (BCY8781) and other pertinent structures, are fully described in Supplementary Chemical Structures.

In vitro binding profile and selectivity

SPR studies showed BT8009 bound human Nectin-4 (hNectin-4) extra-cellular domain (ECD) with a K_D of 2.5 ±1.3 nmol/L. BT8009 also showed high-affinity binding to endogenous Nectin-4 ECD from mouse, rat and non-human primate, all of which show >90% homology with hNectin-4. High selectivity (K_D > 20 μmol/L) was seen over the other members of the human Nectin-family (hNectins1–3) and the five members of the Nectin-like family (hNecl1–5; all of which show <36% homology with hNectin-4). Other Nectin family members from the non-human species also show ≤36% homology with hNectin-4 and so it was judged unlikely BT8009 would show measurable affinity to these (Supplementary Table S1).

In a Retrogenix-binding screen of 5,528 human plasma membrane proteins and cell surface-tethered secreted proteins (including various transporters, adhesion molecules, enzymes and receptors), the only interaction seen for BCY9565 (the biotinylated Bicycle binder present in BT8009) was with Nectin-4 itself, whereas in a functional cardiac ion assay the Bicycle binder (BCY8126) had no activity on the three tested ion channels (hERG, hNav1.5 and Kv1.5). When combined with the selectivity data over other family members, this indicates the extremely high degree of specificity of the Nectin-4–binding bicycle for hNectin-4

High content imaging–binding studies on cells

BT8009 and the Nectin-4-ADC bound endogenous Nectin-4 expressed on the cell membrane of MDA-MB-468 cells, with "apparent affinities" in the low nmol/L range (12.9 ± 1.1 nmol/L and 0.3 ± 2 nmol/L, respectively). The non-binding homologue BCY8781 showed an affinity >10 μmol/L. As expected, the Nectin-4 ADC showed a greater B_{max}(RFU) than BT8009 (35.2 ± 2.2 and 11.2 ± 1.1) because the anti-MMAE detection antibody identified the higher DAR of the ADC. Unconjugated MMAE showed no affinity for the cells (**Fig. 1**). Experiments were performed at 4°C to minimize internalization and optimize cell surface detection.

In vitro and *in vivo* PK parameters

The chemical scaffold and incorporation of non-coded amino acids reduce metabolic lability of BTCs. BT8009 is metabolically stable

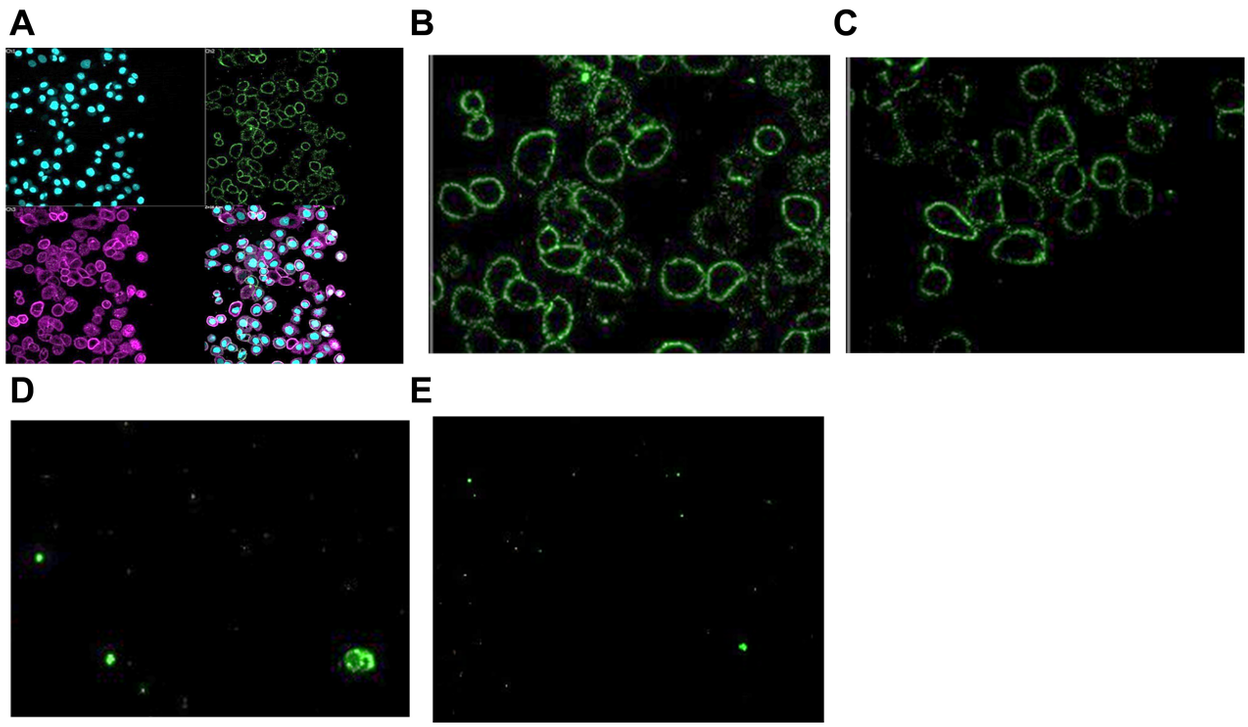

Figure 1.
High content imaging showing anti-MMAE mAb staining after incubation of MDA-MB-468 cells with test agent (each at 1 µmol/L) $n = 4–8$; **A,** Composite showing nuclei stained with DAPI (Cyan), membrane marker (purple) anti-MMAE mAb (green); **B,** with 1 µmol/L Nectin-4 ADC; **C,** with 1 µmol/L BT8009; **D,** with 1 µmol/L MMAE; **E,** with non-binding BTC (BCY8781).

in vitro, in plasma and whole blood, hepatocytes and microsomes from rat, NHP and human. The low intrinsic clearance in hepatocytes and microsomes extrapolate to low estimates of metabolic clearance. *In vitro* stability in mouse plasma was substantially less than the other species, likely due to metabolism by Ces1c, as reported for some ADCs (26, 27). Plasma protein binding for BT8009 was low across these species ($fu_{,P} = 0.12–0.21$; Supplementary Table S2).

BTCs show a pharmacokinetic profile more comparable with small molecules than antibodies. In PK studies in rat and mouse, and TK studies in the NHP, BT8009 conformed with this profile having short terminal half-lives and moderate (higher than plasma volume) volumes of distribution typical for a small conjugate able to freely penetrate tissue. Low levels of unconjugated circulating MMAE were detected from BT8009. Plasma MMAE levels in mouse were higher than the other two species, likely due to the circulating Ces1c in mouse. Circulating parent and MMAE levels are shown in Supplementary Fig. S1 and pharmacokinetic parameters for BT8009 and MMAE are shown in Supplementary Table S3. Literature values for EV are included showing longer $t_{1/2}$, slower clearance rates and much lower volumes of distribution for the ADC.

Tumor MMAE accumulation after BT8009, was assessed in three CDX models (NCI-H292, MDA-MB-468, and NCI-H322). After administration of BT8009 peak tumor concentrations of total MMAE were rapidly attained within 2–4 hours, followed by a small decline in tumor concentrations, as BT8009 and free MMAE cleared from the tumor. Overall MMAE was retained at high levels in the tumor for the duration of the experiments (24–72 hours). This persistent tumor retention of MMAE was in marked contrast with plasma parent BT8009 or free MMAE that showed rapid plasma clearance, and therefore transient systemic exposure, and to muscle that showed minimal MMAE retention in the two models in which muscle was collected (**Fig. 2**).

In vivo mechanism of action and antitumor activity

BT8009 demonstrated dose-related effects on tumor growth in CDX and PDX models over the range 1–3 mg/kg when administered qw (**Fig. 3**). Full tumor regressions were routinely achieved in both models with 3 mg/kg, with no tumor regrowth in subsequent weeks off treatment. Stable disease was delivered by 2 mg/kg and at this dose, in the PDX model, tumor growth resumed after drug cessation. In both models animals from the vehicle treated group were treated with 3 mg/kg BT8009 when tumors reached approximately 800 mm^3 or 1,000 mm^3. Profound tumor regression was rapidly initiated in response. In the majority of studies 3 mg/kg, qw, was adopted as the standard dosing regimen.

Association of target expression with BT8009 antitumor activity was confirmed as an important aspect of BT8009 mechanism of action. A variety of CDX and PDX models were preselected on the basis of differing Nectin-4 expression levels, assessed by FACS and/or IHC. BT8009 was dosed at 3 mg/kg i.v. qw. There was a clear association between degree of tumor regression and level of Nectin-4 expression (**Fig. 4A**), except for the HT1376 line (discussed below). Target dependence was further tested in a screen of lung PDX models in which Nectin-4 was assessed by IHC retrospectively (**Fig. 4B**). Nectin-4 expression levels and BT8009 antitumor activity were clearly associated across these datasets. Xenografts with little or no Nectin-4 expression showed minimal response to BT8009, displaying either no effect on, or at best, a reduction in tumor

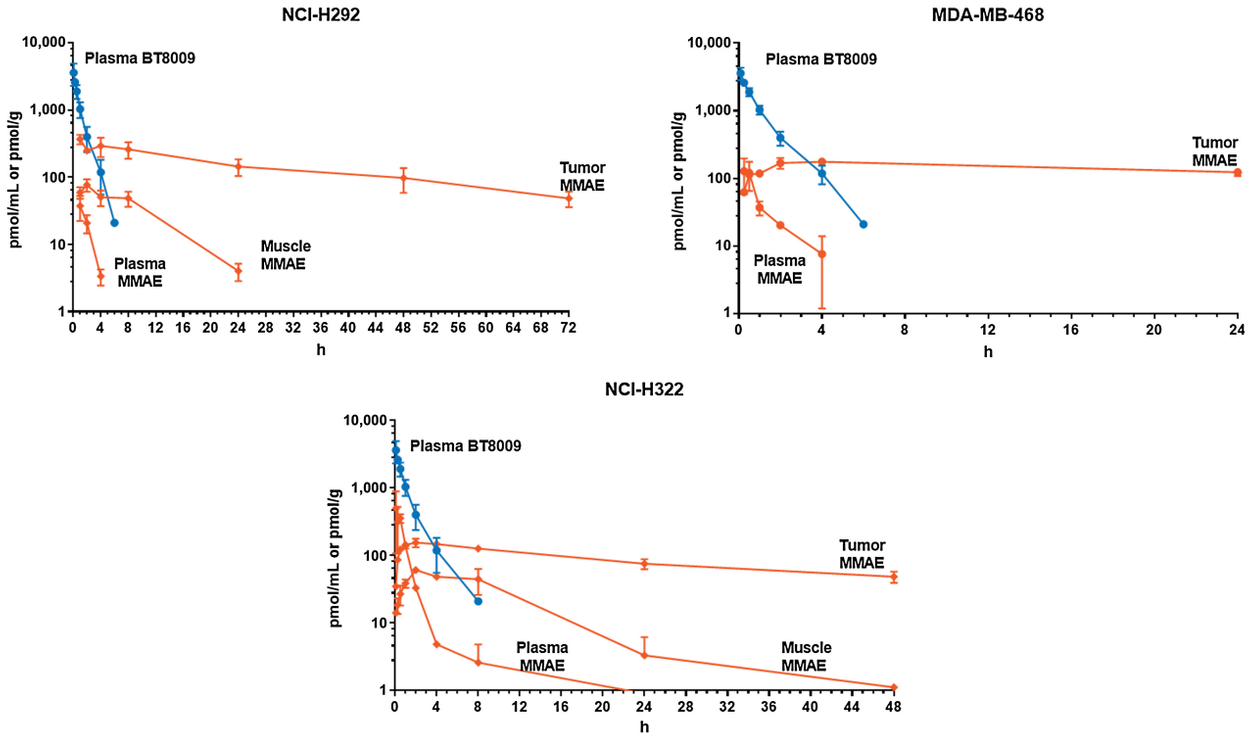

Figure 2.

PK profile of BT8009 and MMAE in three mouse xenograft models. MMAE is rapidly cleared from plasma but retained in tumor substantially longer. Error bars indicate SD of $n = 3$ per timepoint.

growth rate. As Nectin-4 expression levels increased the degree of antitumor activity increased.

Whereas Nectin-4 expression is a key element in driving optimal tumor regression, other factors also contribute to level of response (Supplementary Fig. S2). In HT1376 xenografts, BT8009 treatment evoked a reduction in tumor growth rate, without tumor regression. Nectin-4 membrane expression in HT1376 tumor cells was extremely heterogenous based on FACS and IHC, with some cells expressing no

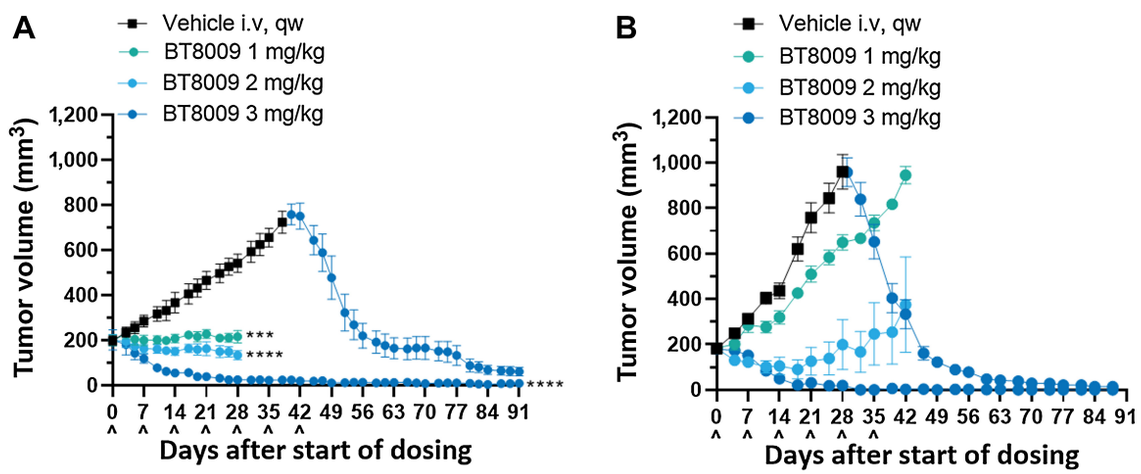

Figure 3.

BT8009 shows dose-related antitumor activity in; **A,** A CDX (triple-negative breast cancer) xenograft model. Dosing of the 3 mg/kg initial treatment group was ceased on day 42. Vehicle-treated animals were switched to 3 mg/kg BT8009 qw on day 40 and then 5 mg/kg qw on day 75. **B,** a PDX (non–small cell lung) xenograft model. Dosing of the 3 mg/kg initial treatment group was ceased on day 45. Vehicle-treated animals were switched to 3 mg/kg BT8009 qw on day 36. Tumor volumes are shown as mean ± standard error of the mean ($n = 3$–5) and statistical analysis performed with ordinary one-way ANOVA with Tukey's *post hoc* test for multiple comparisons ***, $P < 0.001$ and ****, $P < 0.0001$.

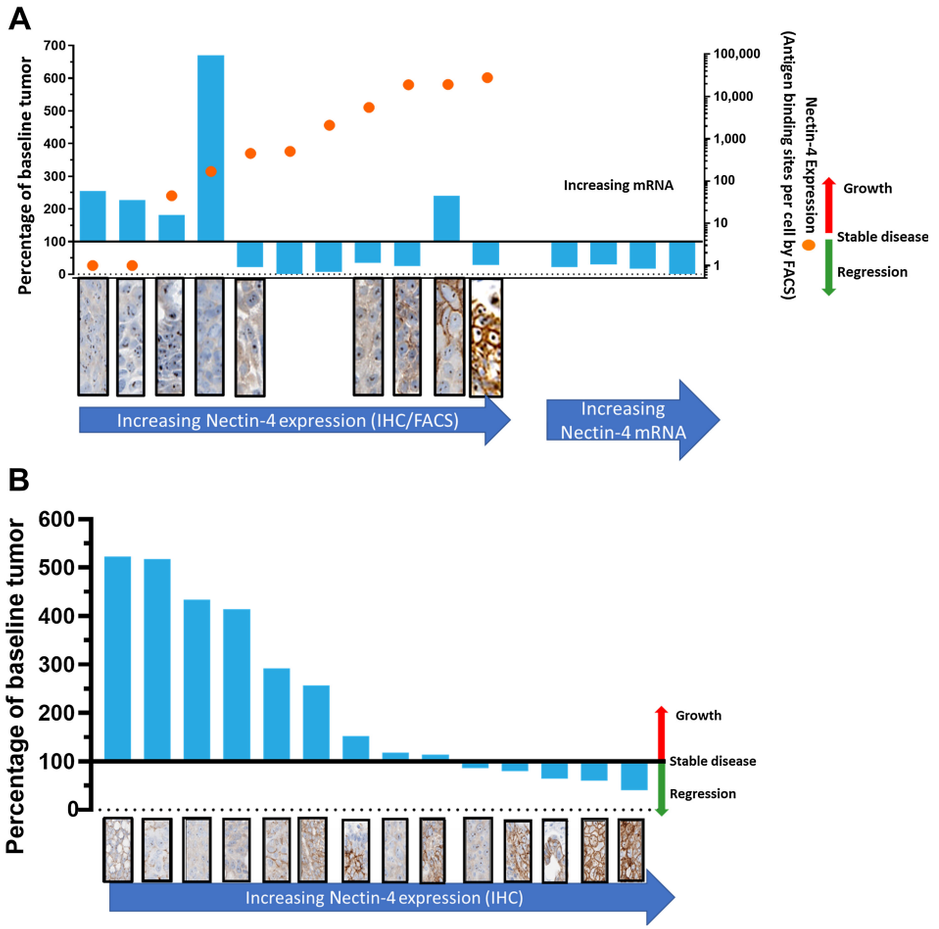

Figure 4.

Relationship between BT8009 antitumor activity and target expression in CDX and PDX models; **A,** The percentage of change from initial tumor volume (blue columns–values above 100% indicate tumor growth, below 100% indicate tumor regression) and Nectin-4 expression assessed by FACS (orange circles, indicating antigen-binding sites per cell). FACS and IHC data are not available for 4 PDX models on right of **A**. IHC for Nectin-4 (stained brown) is shown in panels below the cell type; **B,** The percentage of change from initial tumor volume and Nectin-4 expression, assessed by IHC, in 14 NSCLC PDX models. Animals were dosed with 3 mg/kg BT8009, qw, in all studies.

membrane Nectin-4. *In vitro*, HT1376 are less sensitive to administered MMAE, with lower cathepsin B secretion. This impacts the TME cleavage of BT8009 and efficacy in killing Nectin-4–expressing cells directly, and non-expressing cells by the bystander effect. Even at high concentrations EV only kills approximately 75% of HT1376 cells *in vitro* (28). The A549 cell line, lacks Nectin-4 expression, but with comparable MMAE sensitivity with other lines and high cathepsin B secretion showed tumor growth rate reduction, but without any regression in response to BT8009. However, tumor regression was seen in tumor types showing membrane expression of Nectin-4, good sensitivity to MMAE and high levels of cathepsin B secretion (NCI-H292 and MDA-MB-468), emphasizing the importance of the combination of these factors for optimal tumor regression with BT8009.

We also addressed the requirement of Nectin-4 binding for optimal antitumor response in the MDA-MB-468 TNBC CDX model. BT8009 was co-administered with a 130-fold excess of BCY8234, an MMAE-free analogue of BT8009. Co-administration of trastuzumab with ado-trastuzumab emtansine enhances antitumor activity through overcoming binding site barrier (4); however, co-administration of excess BCY8234 attenuated the response to BT8009 (**Fig. 5A**) likely by blocking cell surface Nectin-4 preventing localized release of toxin by TME immediately adjacent to the cell surface and/or preventing internalization of BT8009 (should this occur). This observation strongly suggests that the binding site barrier is less influential for BT8009 in these studies.

The response to the non-binding analogue BCY8781 was assessed in the same study. Because BCY8781 penetrates the tumor and liberates toxin in the TME, a degree of antitumor activity is expected. The scale and rate of tumor regression with BCY8781 was demonstrably less than that seen with the equivalent dose of BT8009 (**Fig. 5B**) but was strikingly similar to the response to BT8009 in the presence of excess toxin free binder. In a PDX model, BT8009 consistently showed greater effect than the non-binder, the best response seen with BCY8781 being stable disease, whereas complete tumor regressions were seen with BT8009 (**Fig. 5C–E**).

The dependence on membrane expression for optimal tumor regression across multiple models; the attenuation of efficacy with co-administered toxin-free peptide and the reduced effect seen with the non-binding BTC homologue, clearly demonstrate the requirement for target expression, the presence of appropriate cleavage enzymes within the TME, as well as sensitivity of tumor cells to MMAE, for maximal activity of BT8009.

A key aspect of BTCs observed in preclinical testing is their significant tissue penetration that we believe is due to their low molecular weight. Xenograft studies were performed to verify that in larger tumors BT8009 showed comparable activity with smaller tumors, and in two models MMAE content, per g tumor, was assayed and found to be the same for large (~1,000 mm^3) and small tumors (~200 mm^3), indicating good tumor penetration of BT8009. BT8009 showed robust activity against tumors in multiple models, evoking tumor regression in tumors ranging in size from approximately 200 to

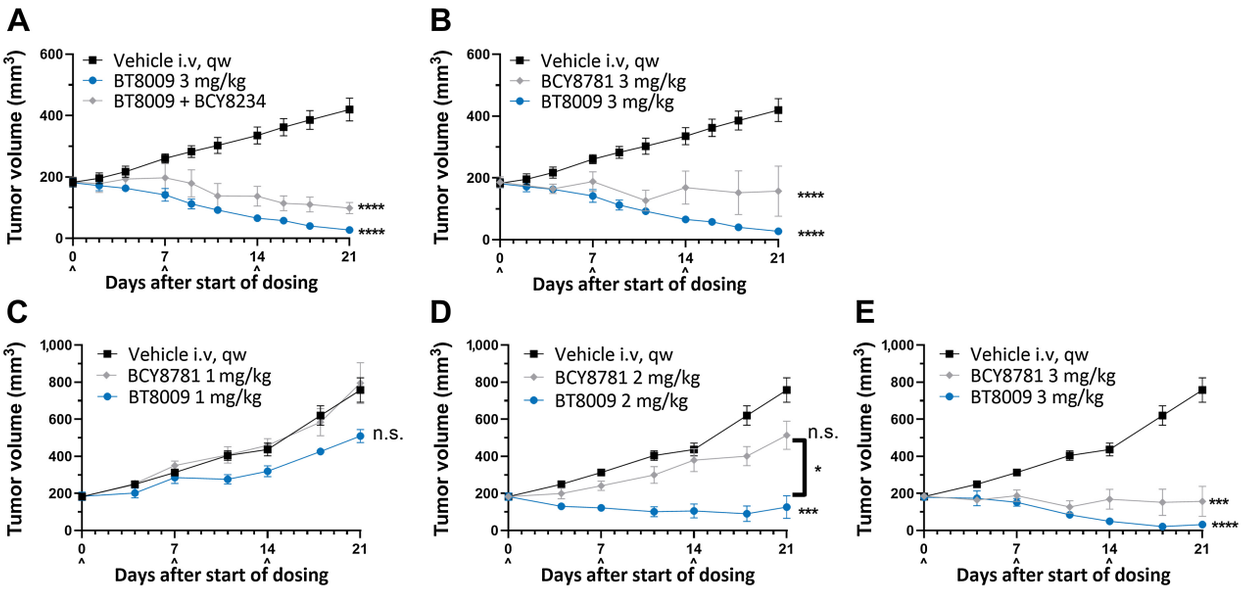

Figure 5.

A, In the MDA-MB-468 xenograft BT8009 was dosed alone or in combination with an excess of unconjugated bicycle, BCY8234, antitumor activity was attenuated by the unconjugated peptide. BT8009 showed significant difference from vehicle from day 7 onwards, BT8009 with BCY8234 showed significant difference from vehicle from 14 days onwards. **B,** In the same study the non-binding BTC homologue BCY8781 failed to produce comparable effect with BT8009, with significant difference from vehicle from day 9 onwards. BT8009 versus BCY8781 were significantly different on days 18 and 21. **C–E,** In the LU-01–0412 PDX model, BT8009 consistently showed greater tumor regression than the non-binding homologue BCY8781 at equivalent doses. Tumor volumes are shown as mean ± standard error of the mean ($n = 3$–5) and statistical analysis performed with ordinary one-way ANOVA with Tukey's *post hoc* test for multiple comparisons n.s., non-significant; * $P < 0.05$; *** $P < 0.001$; and **** $P < 0.0001$.

1,000 mm^3. Rates of regression were no slower in larger tumors, with rapid regression initiated even after the first dose. These data support a deep penetration of BT8009 throughout the tumor from the first dosing event (Supplementary Fig. S3).

BT8009 was effective in producing robust tumor regression in large and small tumors across a variety of dosing paradigms. In the NCI-H322 (NSCLC, non–small cell lung cancer) model, significant response was seen when BT8009 was given twice a week, once a week or once every two weeks, potentially supporting the utility of multiple dosing regimens in the clinical arena (Supplementary Fig. S4).

Comparison with a Nectin-4 ADC

A Nectin-4 ADC, modeled on EV, was tested alongside BT8009 in several CDX and PDX models. ADC doses used in these studies were based on doses of EV used in existing literature (13) where marked tumor regression was seen with a single dose of either 10 or 4 mg/kg, or 3 mg/kg given every 4 days, depending on model. A second Nectin-4 ADC (N41mab-vcMMAE) showed tumor regression in TNBC models at 2.5 or 10 mg/kg as two doses 4 days apart (17). Notably, BT8009 with a molecular mass of 4171 at 3 mg/kg BT8009 delivers 7.2×10^{-7} moles of MMAE/kg, whereas 10 mg/kg of the in house Nectin-4 ADC (mass 152 kDa; DAR $\sim$ 4.0) delivers 2.6×10^{-7} moles of MMAE/kg.

In several different CDX or PDX models BT8009 showed equivalent or superior tumor regression activity to the Nectin-4 ADC, despite often using higher ADC doses than those described in the literature. In a NSCLC model, BT8009 provided more rapid and greater tumor regression than the ADC (**Fig. 6A** and **B**). In a TNBC model, the regression seen with BT8009 was again more rapid (**Fig. 6C**). In a PDX NSCLC model, whereas rate and degree of regression were comparable for the ADC and BT8009, the BT8009 cohort showed no regrowth out to 35 days after treatment cessation, but the ADC group showed tumor regrowth from drug cessation. This suggests incomplete tumor killing by the ADC but not the BTC (**Fig. 6D**). Strikingly, in a head and neck PDX model (showing moderate Nectin-4 IHC), BT8009 halted tumor growth at 3 mg/kg whereas 5 mg/kg evoked tumor regression. In comparison the ADC, dosed initially at 5 mg/kg and subsequently 10 mg/kg, minimally reduced tumor growth rate. ADC-treated mice subsequently dosed with 3 mg/kg BT8009, showed arrest of tumor growth and initiation of regression that was accentuated when the BTC dose was increased to 5 mg/kg BT8009, indicating retained sensitivity to the MMAE (**Fig. 6E**). In other xenograft models, we saw comparable effects with the two agents, but in no models were antitumor activity seen with the ADC and not with BT8009.

General toxicology studies

BT8009 displayed a subset of toxicities, typically associated with MMAE and the maximum-tolerated dose (MTD) was determined to be 5 mg/kg in the rat and 1.5 mg/kg in the non-human primate, when administered as 5 weekly doses (both species). Dose-limiting toxicity was attributed to the effects of the MMAE payload with decreases in red blood cell parameters (erythrocyte and leucocyte counts), neutropenia and histopathological changes observed in those tissues associated with a high mitotic rate (e.g., bone marrow and lymphoid tissue). At doses up to and including the MTD, there were no significant GI, liver or kidney macroscopic or microscopic effects observed.

Discussion

BTCs are new therapeutic modality that shows a very different pharmacokinetic and structural profile to classic ADCs, whereas

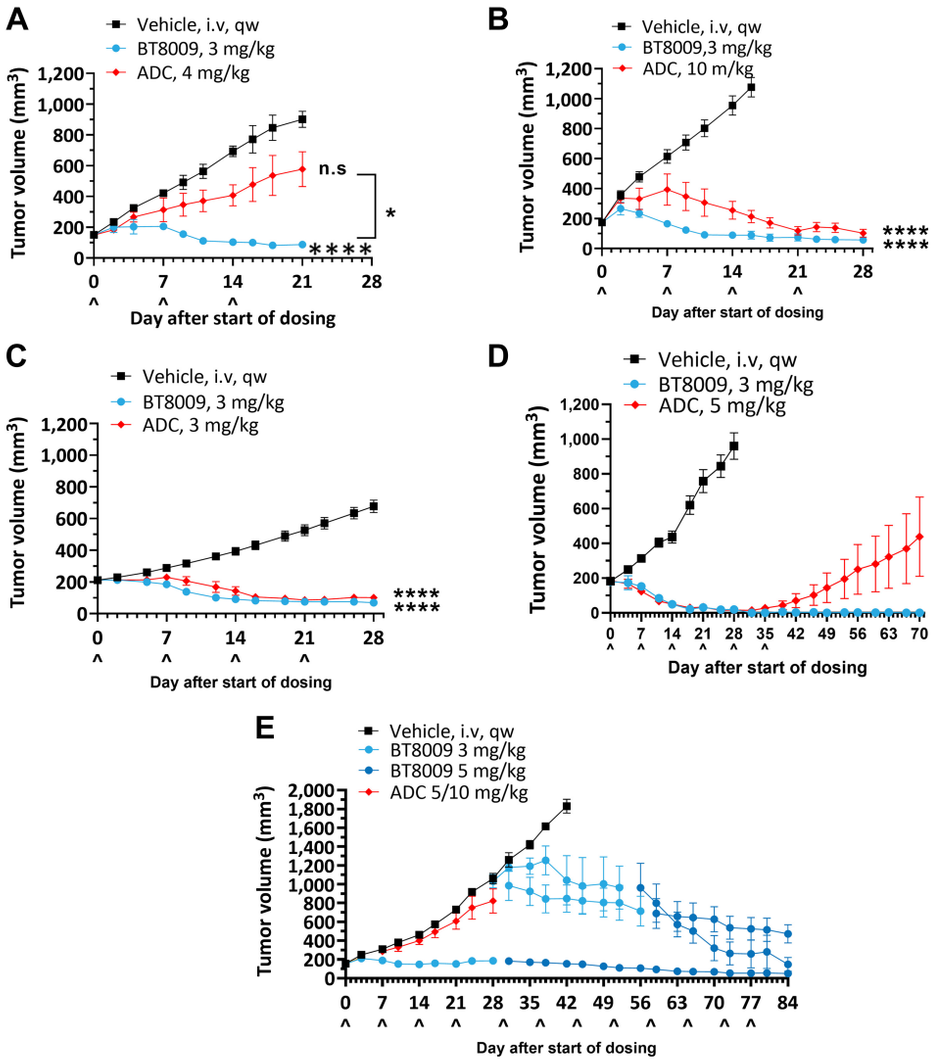

Figure 6.

Head-to-head studies with the Nectin-4 ADC. **A** and **B,** Dose response to ADC in NSCLC CDX (NCI-H292) with high dose showing slower tumor regression than with BT8009; **C,** Response in TNBC CDX (MDA-MB-468) showing slower response to treatment with ADC; **D,** Equivalent regression rate with ADC, but tumor growth resumed on cessation of dosing, indicating incomplete regression in a lung PDX (LU-01-0412), unlike after BT8009; **E,** Lack of effect of ADC in head and neck PDX (HN-13-001) compared with BT8009 efficacy. ADC was dosed at 5 mg/kg on D0 and D7, then increased to 10 mg/kg on D14. ADC-treated tumors remain responsive to BT8009. Tumor volumes are shown as mean ± standard error of the mean (n = 3–16) and statistical analysis performed with ordinary one-way ANOVA with Tukey's *post hoc* test for multiple comparisons n.s., non-significant; *, $P < 0.05$; ***, $P < 0.001$; and ****, $P < 0.0001$.

possessing robust tumoricidal properties. BTCs targeting MT1-MMP and EphA2 are currently in clinical trials (29, 30). BT8009 is the most recent BTC to enter clinical trial (31).

BT8009 is highly selective for Nectin-4 over other nectin family members and an extensive range of cell membrane expressed proteins. It shares the same cleavable linker and toxin combination as EV and can be cleaved by proteases in the TME, releasing cell penetrant MMAE that diffuses into tumor cells, or bystander stromal-supportive cells, evoking cell death, and tumor regression. It shows a robust and dose-dependent antitumor activity in multiple CDX and PDX models, representing lung, breast, bladder, head and neck cancers. Optimal tumor regression is associated with membrane expression of Nectin-4, in conjunction with MMAE sensitivity. Tumor regression rates are comparable for small and large tumors, indicative of deep and rapid penetration throughout the tumor. BT8009 provides tumoricidal activity with several regimens, potentially allowing for clinical titration of dose and dose interval if required.

In head-to-head studies with an ADC modeled on EV, the antitumor activity seen is equivalent, or at times superior, to that obtained with the Nectin-4 ADC, even with higher and/or more frequent ADC administration than previously reported in the literature for EV (13). Whereas extracellular cleavage of ADCs has been reported (32), generally most ADCs are designed for internalization and lysosomal cleavage to release toxin (33), and this is the primary mechanism of action ascribed to EV (13, 18) and N41mab-vcMMAE (17). Toxin subsequently released back into the TME evokes bystander killing. BTCs can be cleaved within the TME making MMAE more freely available for uptake by tumor cells or supportive stromal cells. Furthermore, the BTC may show efficacy where internalization is reduced or where aberrant endocytic processing occurs, mechanisms of ADC resistance. These aspects may explain the response seen with BT8009, but not the ADC, in the head and neck PDX, despite the ADC-treated animals remaining sensitive to later treatment with BT8009.

Systemic administration of BT8009 results in a markedly different pharmacokinetic profile to that expected of an ADC. The high C_{max}, combined with smaller size (4.2 vs. 152 kDa for EV) drives rapid extravasation into the tissue, reflected in a greater volume of distribution (mouse Vd_{ss} = 0.25 L/kg for BT8009 and 0.08 L/kg for EV). Despite this high C_{max}, circulating levels of MMAE are low and both parent BT8009 and MMAE are rapidly cleared from the

circulation, with short terminal plasma half-lives measured in hours rather than days (BT8009 $t_{1/2}$ rat = 0.9 hours; $t_{1/2}$ NHP = 1.7 hours: EV $t_{1/2}$ rat = 1–1.3 days; $t_{1/2}$ NHP = 0.7–1.7 days; EV multidisciplinary review and evaluation).

Long systemic duration partially mitigates the poor tissue penetration of ADCs; however, inherent in sustained exposure is the possibility of increased target dependent and independent toxicity. ADCs may be taken up by off target, receptor mediated, endocytosis, for example, through binding to Fcγ receptors or C type lectin receptors, or by non-specific endocytosis (10). BTCs have no Fc domain liability and are not glycosylated. The Nectin-4–binding Bicycle showed no binding to multiple members of these families in the Retrogenix-binding assay additionally, its shorter circulating plasma half-life would be expected to make it less susceptible to prolonged target independent micro/macro-pinocytosis.

Smaller antibody formats (e.g., diabodies, fabs, ScFvs) have been used to improve extravasation and tumor penetration. Comparison of an anti-CD30 MMAF diabody conjugate with its full IgG–MMAF conjugate showed despite a more rapid clearance (25–34-fold greater) and the diabody showed a third of the potency of the full ADC *in vivo*, but this was comparable with their relative *in vitro* efficacies, suggesting reduced efficacy may be driven by potency differences rather than exposure. Indeed, increasing the diabody dose 3-fold provided equivalent efficacy, demonstrating comparable efficacy can be achieved with smaller formats despite, high clearance (34). Because MMAF is not cell penetrant, efficacy depends on diabody/antibody internalization; making target saturation and internalization rate more influential on efficacy response where the drug conjugate is rapidly cleared from the tumor. BT8009 efficacy may be less susceptible to rapid clearance of parent because it can be rapidly cleaved in the TME to release toxin, without necessarily requiring internalization. This is supported by PK data showing that despite short systemic exposure BT8009 delivers significant MMAE to tumor cells, MMAE peaking in the tumor within two hours and being retained for periods well in excess of the plasma circulation, indicative of rapid tumor cell MMAE uptake and engagement with target.

The toxin peptide ratio of BT8009 is 1:1, ADCs routinely have higher DARs and frequently show heterogeneity in their DAR. This and DAR-dependent sequential deconjugation and ADC clearance, makes clinical pharmacokinetic predictions complex (35). There are further advantages of the lower toxin load per molecule. In xenograft models, decreasing DAR of an ADC, whereas delivering the same overall toxin load, improves efficacy (4), and reduction of DAR from 8 to 4 maintains efficacy whereas increasing therapeutic index (36). A higher DAR, increases the likelihood that more MMAE is delivered to the cell than is required to initiate cell death ("overdosing"), meaning a proportion of the total MMAE load delivered to the tumor is effectively wasted. BT8009's lower toxin ratio means it is possible to deliver a greater number of BT8009 molecules for the same total MMAE load as that commonly seen with ADCs. We believe this promotes distribution of toxin load to the maximum number of tumor cells, reducing "overdosing" of tumor cells and minimizing the impact of the "binding site barrier" on the delivery of toxin into poorly perfused regions of the tumor.

Despite two decades passing since the initial approval of Mylotarg (gentuzumab ozogamicin) and substantial activity in the field, with over 80 ADCs currently being assessed in approximately 150 active clinical trials, there are still only 5 ADCs approved by the FDA for solid tumors (37). BTCs present an opportunity for improving on the targeted delivery of toxin approach. BTCs appear to provide a toxin delivery system with the targeting advantages seen with ADCs, but with a very different PK profile comprising significantly shorter systemic exposure and optimization for rapid tumor penetration. BT8009 is the latest NCE of this class, targeting a tumor antigen that has been clinically validated by the ADC EV. BT8009 shows robust antitumor activity in a wide range of CDX and PDX tumor types, with full tumor regression frequently seen in large and small tumors. The activity seen is comparable, or at times superior, with that seen with a Nectin-4 ADC. BT8009 is currently in a Phase 1/2 multicenter clinical trial across the US, Canada, and Europe, enrolling patients with advanced solid tumors associated with Nectin-4 expression. Interim Phase 1 results published on April 10, 2022 (38) show a 50% confirmed overall response rate and a 75% disease control rate, including one confirmed complete response in eight patients with urothelial cancer dosed at 5.0 mg/m^2 weekly. BT8009 also exhibits a promising preliminary tolerability profile. These emerging clinical data show potential for differentiation from antibody-based approaches.

Authors' Disclosures

M. Rigby reports a patent for WO 2019/243832 pending and WO 2019/243833 pending. G. Bennett reports personal fees from Bicycle Tx Ltd. outside the submitted work. L. Chen reports a patent for WO2019/243832 pending and a patent for WO2019/243833 pending. G.E. Mudd reports a patent for Bicyclic peptide ligands specific for Nectin-4 issued to Bicycle Tx; and Owns stock/stock options in Bicycle Tx Ltd. K. van Rietschoten reports a patent for Bicyclic peptide ligands specific for Nectin-4 issued to Bicycle Tx; as well as reports stock/stock options in Bicycle Tx Ltd. P.U. Park reports other support from Bicycle Therapeutics during the conduct of the study; other support from Bicycle Therapeutics outside the submitted work; as well as P.U. Park has a patent for US11180531B2 issued. J. Lahdenranta reports other support from Bicycle Therapeutics during the conduct of the study. N. Keen reports personal fees and other support from Bicycle Therapeutics during the conduct of the study; personal fees and other support from HotSpot Therapeutics and Kymera Therapeutics outside the submitted work; and an officer of Bicycle therapeutics, reports employment and shareholder. K. Lee reports personal fees from Bicycle Therapeutics outside the submitted work. No disclosures were reported by the other authors.

Authors' Contributions

M. Rigby: Conceptualization, resources, data curation, formal analysis, supervision, validation, investigation, visualization, methodology, writing–original draft, project administration, writing–review and editing. **G. Bennett:** Conceptualization, writing–review and editing. **L. Chen:** Resources, supervision, methodology, writing–review and editing. **G.E. Mudd:** Conceptualization, resources, supervision, methodology, writing–review and editing. **H. Harrison:** Supervision, writing–review and editing. **P.J. Beswick:** Conceptualization, supervision, writing–review and editing. **K. van Rietschoten:** Resources, methodology, writing–review and editing. **S.M. Watcham:** Resources, investigation, methodology. **H.S. Scott:** Resources, formal analysis, validation, investigation, methodology. **A.N. Brown:** Data curation, supervision, methodology, project administration. **P.U. Park:** Conceptualization, supervision. **C. Campbell:** Resources, supervision, methodology. **E. Haines:** Investigation, methodology. **J. Lahdenranta:** Supervision, validation, methodology, writing–review and editing. **M.J. Skynner:** Conceptualization, supervision, funding acquisition, writing–review and editing. **P. Jeffrey:** Conceptualization, formal analysis, supervision, writing–review and editing. **N. Keen:** Conceptualization, supervision, funding acquisition, writing–review and editing. **K. Lee:** Conceptualization, funding acquisition, writing–review and editing.

Note

Supplementary data for this article are available at Molecular Cancer Therapeutics Online (http://mct.aacrjournals.org/).

Received November 5, 2021; revised July 1, 2022; accepted September 9, 2022; published first September 16, 2022.

References

1. Goldenberg DM. Targeting of cancer with radiolabeled antibodies. Prospects for imaging and therapy. Arch Pathol Lab Med 1988;112:580–7.
2. Weinstein JN, Eger RR, Covell DG, Black CDV, Mulshine J, Carrasquillo JA, et al. The pharmacology of monoclonal antibodies. Ann NY Acad Sci 1987;507: 199–210.
3. Ackerman M, Pawlowski D, Wittrup KD. Effect of antigen turnover rate and expression level on antibody penetration tumor spheroids. Mol Cancer Ther 2008;7:2233–40.
4. Cilliers C, Menezes B, Nessler I, Linderman J, Thurber GM. Improved tumor penetration and single-cell targeting of antibody–drug conjugates increases anticancer efficacy and host survival. Cancer Res 2018;78:758–68.
5. Singh AP, Guo L, Verma A, Wong GGL, Thurber GM, Shah DK. Antibody coadministration as a strategy to overcome binding-site Barrier for ADCs: a quantitative investigation. AAPS J 2020;22:28.
6. Ponte JF, Lanieri L, Khera E, Laleau R, Ab O, Espelin C, et al. Antibody co-administration can improve systemic and local distribution of antibody–drug conjugates to increase *in vivo* efficacy. Mol Cancer Ther 2021;20:203–12.
7. Li C, Zhang C, Li Z, Samineni D, Lu D, Wang B, et al. Clinical pharmacology of vc-MMAE antibody–drug conjugates in cancer patients: learning from eight first-in-human phase 1 studies. MAbs 2020;12:1699768.
8. Saber H, Leighton JK. An FDA oncology analysis of antibody–drug conjugates. Regul Toxicol Pharmacol 2015;71:444–52.
9. Zhao H, Atkinson J, Gulesserian S, Zeng Z, Nater J, Ou J, et al. Modulation of macropinocytosis-mediated internalization decreases ocular toxicity of antibody–drug conjugates. Cancer Res 2018;78:2115–26.
10. Mahalingaiah KM, Ciurlionis R, Durbin KR, Yeager RL, Philip BK, Bawa B, et al. Potential mechanisms of target-independent uptake and toxicity of antibody–drug conjugates. Pharmacol Ther 2019;200:110–25.
11. Fabre-Lafay S, Monville F, Garrido-Urbani S, Berruyer-Pouyet C, Ginestier C, Reymond N, et al. Nectin-4 is a new histological and serological tumor associated marker for breast cancer. BMC Cancer 2007;7:73.
12. DeRycke MS, Pambuccian SE, Gilks CB, Kalloger SE, Ghidouche A, Lopez M, et al. Nectin 4 overexpression in ovarian cancer tissues and serum: potential role as a serum biomarker. Am J Clin Pathol 2010;134:835–45.
13. Challita-Eid PM, Satpayev D, Yang P, An Z, Morrison K, Shostak Y, et al. Enfortumab vedotin antibody–drug conjugate targeting Nectin-4 is a highly potent therapeutic agent in multiple preclinical cancer models. Cancer Res 2016; 76:3003–13.
14. Athanassiadou AM, Patsouris E, Tsipis A, Gonidi M, Athanassiadou P. The significance of Survivin and Nectin-4 expression in the prognosis of breast carcinoma. Folia Histochem Cytobiol 2011;49:26–33.
15. Nishiwada S, Sho M, Yasuda S, Shimada K, Yamato I, Akahori T, et al. Nectin-4 expression contributes to tumor proliferation, angiogenesis and patient prognosis in human pancreatic cancer. J Exp Clin Cancer Res 2015;34:30.
16. Deng H, Shi H, Chen L, Zhou Y, Jiang J. Over-expression of Nectin-4 promotes progression of esophageal cancer and correlates with poor prognosis of the patients. Cancer Cell Int 2019;19:106.
17. M-Rabet M, Cabaud O, Josselin E, Finetti P, Castellano R, Farina A, et al. Nectin-4: a new prognostic biomarker for efficient therapeutic targeting of primary and metastatic triple-negative breast cancer. Ann Oncol 2017;28:769–76.
18. Liu BA, Olson D, Snead K, Gosink J, Tenn E-M, Zaval M, et al. Additional mechanisms of action of enfortumab, and anti–Nectin-4 ADC demonstrating bystander effect and immunogenic cell death antitumor activity in models of urothelial carcinoma. Cancer Res 2020;80:5581.
19. Bennett G, Lutz R, Park P, Harrison H, Lee K. Development of BT1718, a novel bicycle–drug conjugate for the treatment of lung cancer. Cancer Res 2017;7:1167.
20. Bennett G, Brown A, Mudd G, Huxley P, van Rietschoten K, Pavan S, et al. MMAE delivery using the bicycle toxin conjugate BT5528. Mol Cancer Ther 2020;19:1385–94.
21. Mosesson Y, Mills GB, Yarden Y. Derailed endocytosis: an emerging feature of cancer. Nat Rev Cancer 2008;8:835–50.
22. Abella JV, Park M. Breakdown of endocytosis in the oncogenic activation of receptor tyrosine kinases. Am J Physiol Endocrinol Metab 2009;296:E973–84.
23. Hammood M, Craig AW, Leyton JV. Impact of endocytosis mechanisms for the receptors targeted by the currently approved antibody–drug conjugates (ADCs)-A necessity for future ADC research and development. Pharmaceuticals 2021; 14:674.
24. Heinis C, Rutherford T, Freund S, Winter G. Phage-encoded combinatorial chemical libraries based on bicyclic peptides. Nat Chem Biol 2009;5:502–7.
25. Mudd G, Scott H, Chen L, van Rietschoten K, Ivanova-Berndt G, Dzionek K, et al. J Med Chem 2022 (in press).
26. Ubink R, Dirksen EHC, Rouwette M, Bos ES, Janssen I, Egging DF, et al. Unraveling the interaction between carboxylesterase 1c and the antibody–drug conjugate SYD985: improved translational PKPD by using CES1c knockout mice. Mol Cancer Thera 2018;17:2389–98.
27. Dorywalska M, Dushin R, Moine L, Farias SE, Zhou D, Navaratnam T, et al. Molecular basis of valine-citrulline-PABC linker instability in site-specific ADCs and its mitigation by linker design. Mol Cancer Ther 2016;15958–70.
28. Chu C, Sjöström M, Egusa EA, Gibb E, Badura ML, Koshkin VS, et al. Heterogeneity in Nectin-4 expression across molecular subtypes of urothelial cancer mediates sensitivity to enfortumab vedotin. Clin Cancer Res 2021;27: 5123–30.
29. NCT03486730. BT1718 in patients with advanced solid tumours.
30. NCT04180371. Study BT5528–100 in patients with advanced solid tumors associated with EphA2 expression.
31. NCT04561362. Study BT8009–100 in subjects with nectin-4 expressing advanced solid tumors malignancies.
32. Gebleux R, Stringhini M, Casanova R, Soltermann A, Neri D. Non-internalizing antibody–drug conjugates display potent anticancer activity upon proteolytic release of monomethyl auristatin E in the sub-endothelial extracellular matrix. Int J Cancer 2017;1401670–9.
33. Jin Y, Schladetsch M, Huang X, Balunas MJ, Weimer AJ. Stepping forward in antibody–drug conjugate development. Pharmacol Ther 2022;229:107917.
34. Kim KM, MCdonagh CF, Westendorf L, Brown LL, Sussman D, Feist T, et al. Anti-CD30 diabody–drug conjugates with potent antitumor activity. Mol Cancer Ther 2008;7:2486–97.
35. Sukumaran S, Zhang C, Leipold DD, Saad OM, Xu K, Gadkar K, et al. Development and translational application of an integrated, mechanistic model of antibody–drug conjugate pharmacokinetics. AAPS J 2017;19:130–40.
36. Hamblett KJ, Senter PD, Chace DF, Sun MMC, Lenox J, Cerveny CG, et al. Effects of drug loading on the antitumor activity of a monoclonal drug conjugate. Clin Cancer Res 2004;10;7063–70.
37. Dean AQ, Luo S, Twomey JD, Zhang B. Targeting cancer with antibody–drug conjugates: promises and challenges. MAbs 2021;13:1951427.
38. McKean M, Baldini C, Verlingue L, Doger B, Falchook G, Italiano A, et al. BT8009–100 phase I/II study of novel bicyclic peptide and MMAE conjugate BT8009 in patients with advanced malignancies associated with nectin-4 Expression. ASCO 2022, April 8–13, Abstract nr. CT025.